Structure and Properties of Composites of Polyethylene or Maleated Polyethylene and Cellulose or Cellulose Esters

P. M. Kosaka,[1] Y. Kawano,[1] H. M. Petri,[2] M. C. A. Fantini,[3] D. F. S. Petri[1]

[1]*Instituto de Química, Universidade de São Paulo, Avenida Professor Lineu Prestes 748, 05508-900, São Paulo, SP, Brazil*
[2]*Thermo Electron Corporation, P.O. Box 26027, 05513-970 São Paulo, SP, Brazil*
[3]*Instituto de Física, Universidade de São Paulo, P.O. Box 66318, 05315-970, São Paulo, SP, Brazil*

Received 8 February 2006; accepted 15 May 2006
DOI 10.1002/app.24836
Published online in Wiley InterScience (www.interscience.wiley.com).

ABSTRACT: Composites of linear low-density poly(ethylene-*co*-butene) (PE) or maleated linear low-density poly (ethylene-*co*-butene) (M-PE) and cellulose (CEL), cellulose acetate (CA), cellulose acetate propionate (CAP), or cellulose acetate butyrate (CAB) were prepared in an internal laboratory mixer with 20 wt % polysaccharide. The structure and properties of the composites were studied with tensile testing, dynamic mechanical thermal analysis, differential scanning calorimetry, extraction with a selective solvent, Raman spectroscopy, and X-ray diffraction. Composites prepared with M-PE presented yield stress and elongation values higher than those of composites prepared with PE, showing the compatibilizer effect of maleic anhydride. Dynamic mechanical thermal analysis performed for M-PE–CEL, M-PE–CA, M-PE–CAP, and M-PE–CAB composites showed one glass-transition temperature (T_g) close to that observed for pure M-PE, and for M-PE–CAP, another T_g lower than that measured for the polysaccharide was observed, indicating partial mutual solubility. These findings were confirmed by the extraction of one phase with a selective solvent, gravimetry, and Raman spectroscopy. X-ray diffraction showed that the addition of CEL, CA, CAP, or CAB had no influence on the lattice constants of PE or M-PE, but the introduction of the reinforcing material increased the amorphous region.
 J Appl Polym Sci 103: 402–411, 2007

Key words: composites; polyethylene (PE); polysaccharides; solid-state structure; structure-property relations

INTRODUCTION

Recent studies on natural-filler/thermoplastic composites have described the use of natural fibers as low-cost reinforcing fillers in several thermoplastics. A good number of automotive components previously made with glass-fiber composites are now being manufactured with environmentally friendly composites.[1] These composites have received attention from industry because of the thermoplastic nature of natural-fiber/thermoplastic composites, which allows the processing of the composites with traditional processing techniques and the recycling of the resultant products at the end of their useful life or waste.[2] When natural fibers are incorporated into polymer composites, they are of particular interest because they are abundant, renewable, and biodegradable and therefore contribute to the sustainability of world resources.[3–6]

The basic condition for the application of fiber-reinforced composites is perfect adhesion between the components. Without adhesion, the principle of fiber-reinforced systems would not work; that is, the strong fiber carries the load, whereas the matrix distributes and transfers it from one fiber to another.[7] Excessively strong adhesion leads to a rigid composite, whereas in the case of weak adhesion, the aforementioned principle does not work, so the strength at adhesion must be set to an optimum value. Because of the inherently poor compatibility between hydrophilic natural fibers and hydrophobic thermoplastics, functional groups must be incorporated onto the fiber surface[8–10] or into the polymeric matrix.[10–12] One of the most common matrix modifications is the grafting of maleic anhydride (MA) to polyolefins, which increases the compatibility through the esterification between the MA groups and the hydroxyl groups of cellulose (CEL).[11–18] The compatibilization is expected to take place in the polyolefin amorphous phase.[11–13]

Cellulose esters such as cellulose acetate (CA), cellulose acetate propionate (CAP), and cellulose acetate butyrate (CAB) are thermoplastic materials

Correspondence to: D. F. S. Petri (dfsp@iq.usp.br).
Contract grant sponsor: Conselho Nacional de Desenvolvimento Cientifico e Tecnológico.
Contract grant sponsor: Fundação de Amparo à Pesquisa do Estado de São Paulo.

TABLE I
Polysaccharide Characteristics

Sample	Mean length (mm)	Mean diameter (mm)	Weight-average molecular weight (g/mol)[a]	Degree of substitution[a,b]			
				Acetate	Propionate	Butyrate	Hydroxyl
CA	0.06 ± 0.02	0.02 ± 0.01	100,000	2.8	—	—	0.2
CAP	0.06 ± 0.03	0.02 ± 0.01	25,000	0.2	2.3	—	0.5
CAB	0.06 ± 0.01	0.010 ± 0.005	20,000	0.95	—	1.65	0.4

[a] Data supplied by Eastman Chemical Co.
[b] Defined as the average number of hydroxyl groups substituted per anhydroglucose unit.

produced through the esterification of CEL.[18] CAB and CAP are less hydrophilic than CEL or CA. In this work, systematic studies have been performed to determine the effect of the polysaccharide type on the structure and properties of composites with linear low-density poly(ethylene-*co*-butene) (PE) or maleated linear low-density poly(ethylene-*co*-butene) (M-PE). The experimental strategy involved mechanical tests, scanning electron microscopy (SEM), differential scanning calorimetry (DSC), dynamic mechanical thermal analysis (DMTA), extraction with a selective solvent, Raman spectroscopy, and X-ray diffraction (XRD).

EXPERIMENTAL

Materials

PE with a melt flow index of 1.80 g/10 min was kindly supplied by Politeno (São Paulo, Brazil). Benzoyl peroxide (BPO; molecular weight = 242.23 g/mol) and MA (molecular weight = 98.06 g/mol) were purchased from Vetec (Rio de Janiero, Brazil) and used without further purification. CA (CA-398-3), CAP (CAP-482-0.5), and CAB (CAB-381-0.5) were kindly supplied by Eastman Chemical Co. (São Paulo, Brazil). Table I shows the cellulose ester characteristics with the corresponding codes. Short CEL fibers (mean diameter = 0.030 ± 0.008 mm, length = 0.13 ± 0.07 mm) were purchased from Fluka (Buchs SG, Switzerland; 9004-34-6). The mean diameters and lengths of all polysaccharides were measured with a Carl Zeiss Axioplan 2 optical microscope (Montpelier, Vermont) equipped with Leica Q550 IW image analyzer software (Montpelier, Vermont).

Methods

Reactive processing and compounding

PE (40 g) was melted in a Haake Polylab R600 internal laboratory mixer (Thermo Electron GmbH, Karlsruhe, Germany) at 150°C and 80 rpm. After 5 min, MA (4 g) and BPO (0.04 g) were added to the melt and mixed for 4 min. Finally, 8 g of CEL, CA, CAP, or CAB (dried in a vacuum oven at 70°C for 10 days) was added and mixed for an additional 26 min. After compounding, the samples were taken out and shaped into small pellets. All processes were carried out without mixer degassing or N_2 purging. Table II shows the codes used for each type of composite.

Sheet preparation

Sheets of composites were prepared by a compression-molding method. The pellets were pressed at 160°C and 150 kgf/cm^2 for 10 min with a Marconi pneumatic press (Piracicaba, Brazil). The sheet thickness was adjusted with a metal frame 1.6 mm thick.

XRD

XRD experiments were performed in a Rigaku diffractometer (Tokyo, Japan) Bragg–Brentano geometry with monochromatized Cu Kα radiation (wavelength = 0.154 nm) at 40 kV and 20 mA. X-ray data were collected from the 2θ range of 10–40° with a step scanning mode of 0.05° and time intervals of 10 s for 1.6-mm-thick sheets of each sample.

DSC

DSC curves were obtained in a THASS XP-10 apparatus (Friedberg, Germany). Two runs were performed for each sample in closed Al crucibles with about 7.5 mg of the samples under a dynamic N_2 atmosphere (100 mL/min) with a heating and cooling rate of 10°C/min from 25 to 150°C. After heating, the samples were let to cool up to 25°C, and soon after, the samples were reheated under the same conditions. The second heating was considered for the determination of the melting temperature (T_m), which was determined at the peak. The DSC cell was calibrated with In (T_m = 156.6°C, heat of fusion = 28.59 J/g) and Zn (T_m = 419.6°C, heat of fusion = 111.40 J/g).

DMTA

DMTA was performed in a Triton DMA-2000 apparatus (Friedberg, Germany) at a frequency of 1 Hz

TABLE II
Material and Composite Codes

Sample	Code	T_m (°C)[a]	T_g (°C)[b]
Linear low-density poly(ethylene-*co*-butene)	PE	120	−20[c]
Linear low-density poly(ethylene-*co*-butene) grafted with maleic anhydride	M-PE	120	−20[c]
Cellulose	CEL	—	—
Cellulose acetate	CA	229	184
Cellulose acetate propionate	CAP	184	142
Cellulose acetate butyrate	CAB	160	125
Linear low-density poly(ethylene-*co*-butene)/cellulose	PE–CEL	121	—
Linear low-density poly(ethylene-*co*-butene) grafted with maleic anhydride/cellulose	M-PE–CEL	121	45[d]
Linear low-density poly(ethylene-*co*-butene)/cellulose acetate	PE–CA	121	—
Linear low-density poly(ethylene-*co*-butene) grafted with maleic anhydride/cellulose acetate	M-PE–CA	121	—
Linear low-density poly(ethylene-*co*-butene)/cellulose acetate propionate	PE–CAP	120	—
Linear low-density poly(ethylene-*co*-butene) grafted with maleic anhydride/cellulose acetate propionate	M-PE–CAP	122	43[d]
Linear low-density poly(ethylene-*co*-butene)/cellulose acetate butyrate	PE–CAB	121	—
Linear low-density poly(ethylene-*co*-butene) grafted with maleic anhydride/cellulose acetate butyrate	M-PE–CAB	122	—

[a] Determined by DSC.
[b] Determined by DMTA.
[c] The β relaxation was assigned to the T_g value obtained by DMTA measurements for PE or M-PE.
[d] The β_{mix} relaxation was assigned to the T_g value obtained by DMTA measurements for the composites.

over a temperature range of −100 to 250°C at a scanning rate of 3°C/min. The three-point-bending method was used. The samples were 7.7 mm wide, 1.8 mm thick, and 15.0 mm long.

Tensile tests

Tensile tests were performed for the composite, M-PE, and PE samples according to a standard testing method (ASTM D 638-95). The tensile properties were determined for five samples of the same composition in an Instron 4400R apparatus (Norwood, MA) at room temperature operating at a strain rate of 30 mm/min.

SEM

SEM analyses on the composite cryofractured surfaces were obtained with a Phillips XL30 apparatus. To avoid artifacts due to plastic deformation, the samples were fractured under liquid N_2 before the analysis.

Extraction with a selective solvent followed by Raman spectroscopy

Samples of each composite were weighed in a precision balance (±0.0001 g) and trapped in inert nets, which were introduced into a Soxhlet extractor. PE–CEL and M-PE–CEL composites were treated with xylene at 110°C for 8 h, which was a selective solvent for the polyolefin. The composites prepared with cellulose esters were treated with acetone, which was a selective solvent for the cellulose esters, at 55°C for 8 h. After selective extraction, all samples were dried *in vacuo* at 100°C for 24 h and weighed again.

Raman spectra were obtained with a Renishaw Raman System 3000 (Gloucestershire, UK) with a resolution of 4 cm^{-1} and 64 scans per spectrum. The composites were analyzed before and after the extraction with the selective solvent. The characteristic bands of CH_2 at 1440 cm^{-1} present in the polyolefins, C—O—C bonds belonging to the anhydroglucose ring at 1373 cm^{-1} for CEL, and the carbonyl group at 1740 cm^{-1} for cellulose esters were chosen for analysis. The ratio between the intensity (peak height) corresponding to the polysaccharide characteristic band, I_{1373} or I_{1740}, and the intensity corresponding to the characteristic band of CH_2 at 1440 cm^{-1}, I_{1440}, was considered to complement the gravimetric measurements.

RESULTS AND DISCUSSION

The T_m and glass-transition temperature (T_g) values obtained for pure PE, M-PE, CA, CAP, and CAB (Table II) are in agreement with those reported in the literature[19] or given by the producers.[20] On the basis of these data, the initial temperature for the mixing

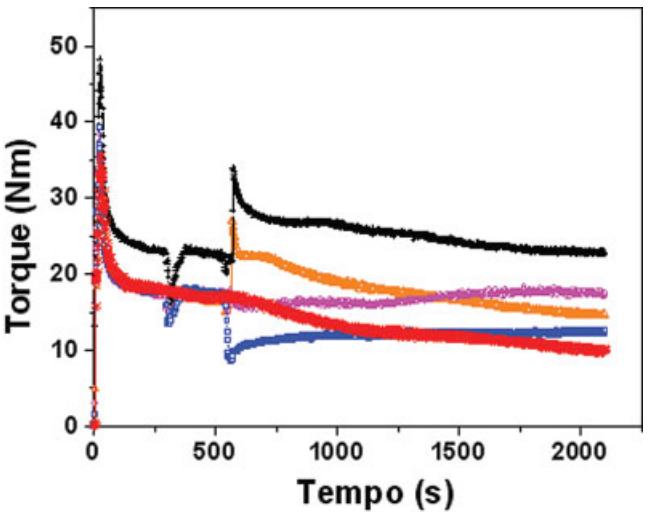

Figure 1 Torque as a function of time for (*) M-PE, (◇) M-PE–CEL, (+) M-PE–CA, (○) M-PE–CAP, and (□) M-PE–CAB. [Color figure can be viewed in the online issue, which is available at www.interscience.wiley.com.]

process was set at 150°C, but because of molecular friction, the temperature rose up to 175 ± 2°C. Figure 1 shows the torque as a function of time for M-PE, M-PE–CEL, M-PE–CA, M-PE–CAP, and M-PE–CAB. The final torque (τ_f) values of the process found for M-PE, M-PE–CEL, M-PE–CA, M-PE–CAP, and M-PE–CAB are 10 ± 1, 15 ± 1, 23 ± 2, 18 ± 2, and 13 ± 1 Nm. Comparing the τ_f values of the process found for M-PE with those observed for the composites, we have found that the addition of CEL, CA, or CAP leads to a significant increase in the τ_f values, whereas the addition of CAB produces a small increase in the τ_f values. Such behavior is expected because at the processing temperature, CAB and the polyolefin are in the molten state, and the viscosity inside the mixing chamber is influenced by the polysaccharide melt viscosity, which is higher than the melt viscosity of the polyolefin. In the case of M-PE–CEL, M-PE–CA, and M-PE–CAP, the presence of the solid filler increases the flow resistance inside the mixing chamber, increasing the τ_f values.

It is well known that the interfacial adhesion between the phases has enormous influence on the mechanical properties of mixtures (blends or composites). The tensile properties obtained for all the samples are presented in Figure 2(a–c). In comparison with PE or M-PE, the addition of polysaccharide leads to an increase in Young's modulus [E; Fig. 2(a)], which overcomes the corresponding standard deviations. Such behavior is expected because it is well known that the modulus of a filled system depends on the properties of the two components, the filler and the matrix.[16,21–23] Thus, the modulus of the reinforcing material (CEL, CA, CAP, or CAB) being higher than the modulus of M-PE or PE, the moduli of the composites are higher than that of the neat polymer. Grafting MA to PE exerts no influence on E obtained for the composites. However, the yield stress (σ_y) values obtained for M-PE–CEL, M-PE–CA, and M-PE–CAP are higher than those σ_y values determined for PE–CEL, PE–CA, and PE–CAP [Fig. 2(b)]. σ_y generally shows a stronger dependence on interfacial adhesion than E; for instance, the tensile yield stress can be well correlated to the interfacial interactions in heterogeneous polymer systems.[16] During the mixing process, an esterification reaction between the —COOH and —C=O groups grafted onto M-PE and the hydroxyl functionality on the polysaccharides can take place, forming a graft copolymer.[8,11,12,24] The

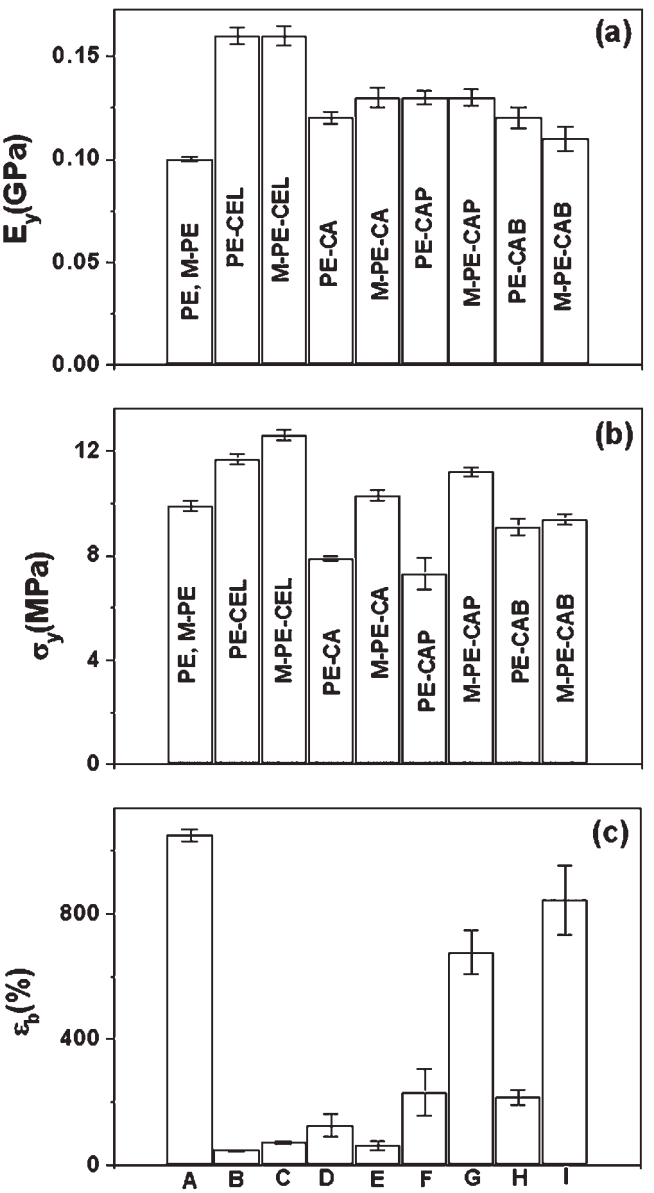

Figure 2 Mechanical properties measured for (A) PE and M-PE, (B) PE–CEL, (C) M-PE–CEL, (D) PE–CA, (E) M-PE–CA, (F) PE–CAP, (G) M-PE–CAP, (H) PE–CAB, and (I) M-PE–CAB: (a) E, (b) σ_y, and (c) ε_b.

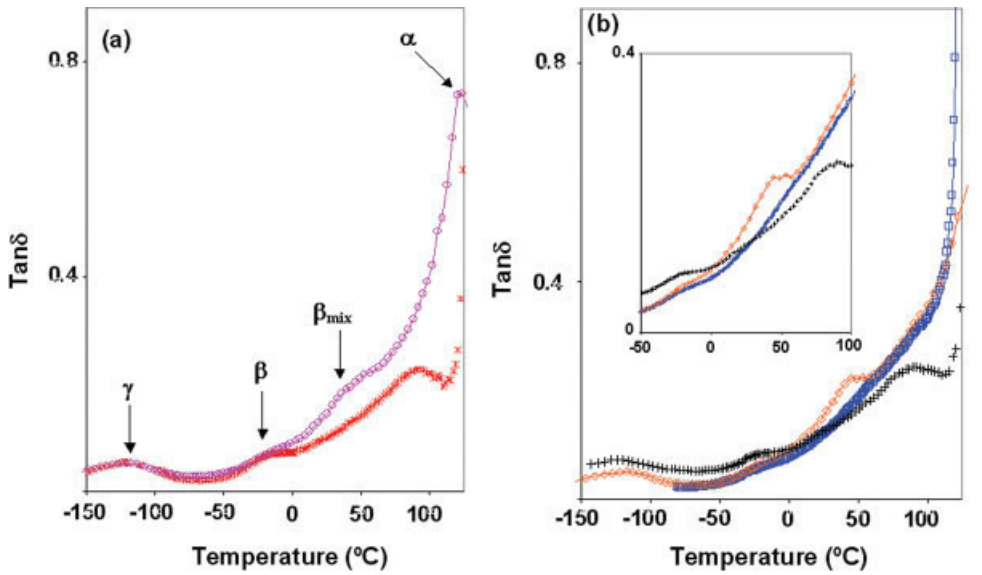

Figure 3 Curves of tan δ as a function of temperature for (a) (*) M-PE and (○) M-PE–CAP and (b) (◇) M-PE–CEL, (+) M-PE–CA, and (□) M-PE–CAB. The insert was added to make reading the β_{mix} transitions easier. [Color figure can be viewed in the online issue, which is available at www.interscience.wiley.com.]

chemical bonding between the two phases promotes better stress transfer from the matrix to the reinforcing phase, leading to a higher tensile strength. This trend can be observed in Figure 2(b), where the highest σ_y values can be found for composites prepared with CEL and CAP, which has the highest number of hydroxyl groups per monomer (degree of substitution for hydroxyl = 0.5). However, in the absence of MA, the σ_y values are low, indicating that the dispersive forces between the hydrophobic polyolefin and the cellulose ester alkyl residues play a marginal role in interfacial adhesion. Another interesting observation is that PE–CEL presents higher tensile strength than the control. This result reflects the contribution of a reinforcing material (CEL) property. In other words, 20 wt % CEL increases the tensile strength of composites prepared with PE because CEL is much stiffer than PE.

In this work, the polysaccharide concentration was set to 20 wt %, which is usual for composites. Recently,[25] we have shown that the addition of 5 or 10 wt % CAB to M-PE leads to materials with tensile properties superior to those obtained for PE or M-PE. However, mixtures with CAB concentrations between 20 and 40 wt % showed tensile behavior comparable to that observed for PE or M-PE. Such an effect has been explained on the basis of the limiting miscibility of up to 10 wt % CAB in the amorphous PE phase, as evidenced by XRD and DSC measurements. The mean σ_y values obtained for PE–CAB and M-PE–CAB [Fig. 2(b)] are lower than those obtained for PE and M-PE, corroborating previous results.[25]

In comparison with pure PE, a dramatic loss in elongation (ε_b) was observed for all samples [Fig. 2(c)]. However, this effect is less pronounced in the presence of M-PE, indicating that the interface modification provides an increase in the toughness and ductility. M-PE–CAP and M-PE–CAB composites present high ε_b values, which are the closest to that obtained for pure PE. This effect might be explained by the CAP and CAB molecular weight values, which are lower than the CA molecular weight. Moreover, CAP and CAB are less crystalline than CA, as shown by the XRD results.

Table II presents T_m and T_g values determined for the composites by means of DSC and DMTA, respectively. With respect to the T_m values, the addition of the reinforcing phase to PE or M-PE leads to an increase of 1 or 2°C, which is negligible.[26] Dynamic mechanical spectra [storage modulus (E'), loss modulus (E''), and tan δ as a function of temperature] were obtained only for composites prepared with M-PE and polysaccharides because they showed better mechanical performance than those prepared with PE. The tan δ curves obtained for PE or M-PE present similar features [Fig. 3(a)]. They exhibit three relaxations, evidenced as peaks, located in the vicinity of −120 (γ), −20 (β), and 122°C (α). The γ peak can be attributed to the relaxing unit consisting of a few chain segments in the amorphous region.[27–31] The β relaxation corresponds to the glass–rubber transition of the amorphous portions, and the temperature is assigned to T_g.[27–31] The α relaxation was first described as vibrational and reorientational motion within the crystals. Later, this relaxation was inter-

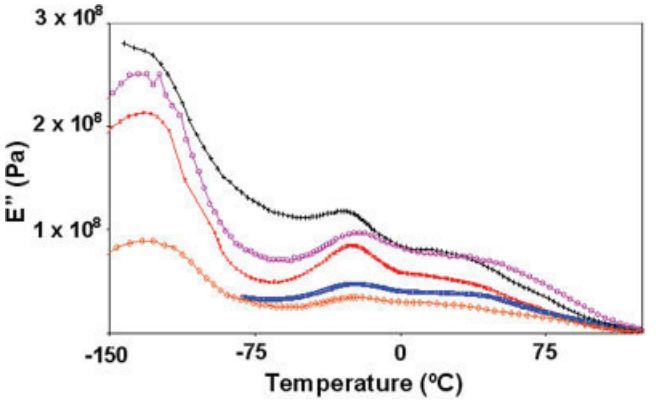

Figure 4 E'' as a function of temperature for (*) M-PE, (◇) M-PE–CEL, (○) M-PE–CAP, (+) M-PE–CA, and (□) M-PE–CAB. [Color figure can be viewed in the online issue, which is available at www.interscience.wiley.com.]

preted as the relaxation of constrained molecules with reduced mobility located near the crystallites.[29] Comparing the spectra obtained for M-PE with those obtained for the composites, one notices that the position of the γ peak remains nearly unchanged. Upon the addition of CEL, CA, CAP, or CAB to M-PE, the position of the β relaxation observed at −20°C for pure M-PE appears at −25 ± 5°C [Fig. 3(a,b)], which might be negligible.[31] However, an additional relaxation, which is here coded β_{mix}, can be observed at a temperature lower than the T_g measured for pure CAP. This relaxation has been assigned to T_g of a miscible phase, indicating partial mutual solubility between M-PE and CAP. The characteristic relaxations also appear as peaks in curves of E'' as a function of temperature (Fig. 4). A relaxation peak close to 80°C has been observed for PE, M-PE, and M-PE–CA. It seems to be characteristic of PE. Upon the addition of polysaccharides to M-PE, the α transition remains practically unchanged.

Figure 5(a,b) presents the curves of E' as a function of temperature obtained for neat M-PE, M-PE–CA, M-PE–CAB, M-PE–CAP, and M-PE–CEL. The addition of CA exerts no effect on the stiffness of M-PE, whereas composites prepared with CAB result in a material softer than M-PE [Fig. 5(a)], corroborating the ε_b behavior observed in Figure 2(c). The system M-PE–CAP is the stiffest, as evidenced by the high E' value, suggesting that the interfacial adhesion between M-PE and CAP is the strongest. This finding corroborates those obtained for σ_y in Figure 2(b).

To obtain materials with improved mechanical properties, the good dispersion of the one phase in the other and strong interfacial adhesion are required. An analysis of the cryofractured surfaces of composites by SEM might provide information about the interfacial adhesion. In the case of PE–CEL, PE–CA, PE–CAP, and PE–CAB composites, the polysaccharide domains present few joint points with the PE matrix and gaps between the polysaccharides domains and the polymeric matrix at the interphase region, indicating poor interfacial adhesion (SEM images are available as supplementary material). On the contrary, SEM micrographs of cryofractured surfaces obtained for M-PE–CEL, M-PE–CA, M-PE–CAP, and M-PE–CAB show multiple points of adhesion between the polysaccharide domains and M-PE matrix and domains better dispersed and smaller, corroborating the superior mechanical behavior observed for the composites containing M-PE (SEM images are available in the supplementary material).

The adhesion between the matrix and filler has been quantitatively evaluated by gravimetric mea-

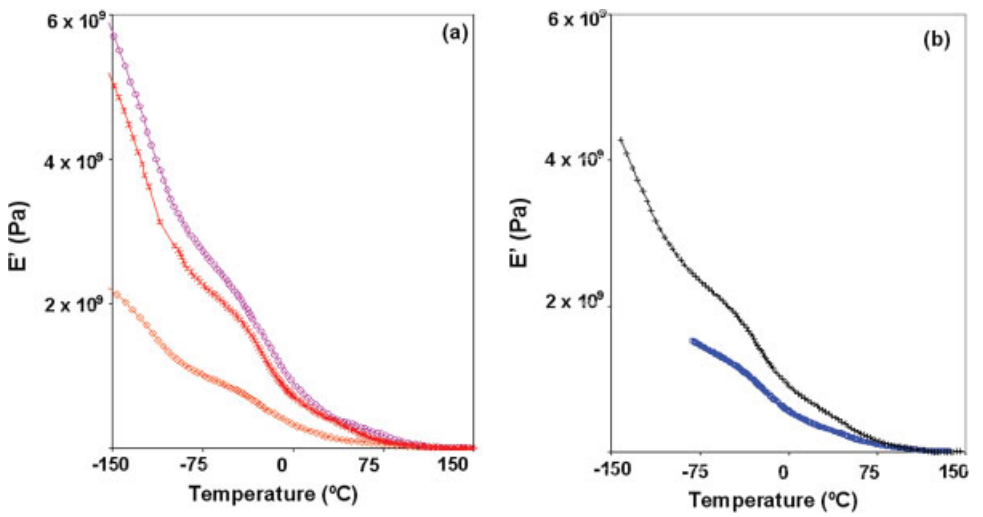

Figure 5 E' as a function of temperature for (a) (*) M-PE, (○) M-PE–CAP, and (◇) M-PE–CEL and (b) (+) M-PE–CA and (□) M-PE–CAB. [Color figure can be viewed in the online issue, which is available at www.interscience.wiley.com.]

TABLE III
Mass Reduction Determined by Gravimetry after Extraction with a Selective Solvent

Sample	Mass reduction after extraction (%)	I_{1373}/I_{1440}[b]		I_{1740}/I_{1440}[b]	
		Before extraction	After extraction	Before extraction	After extraction
PE	0	—	—	—	—
M-PE	0	—	—	—	—
PE–CEL	80 ± 1[a]	0.021 ± 0.001	0.13 ± 0.06	—	—
M-PE–CEL	74 ± 1[a]	0.063 ± 0.003	0.17 ± 0.08	—	—
PE–CA	6.66 ± 0.03	—	—	0.073 ± 0.004	0.042 ± 0.002
M-PE–CA	5.57 ± 0.03	—	—	0.062± 0.003	0.044 ± 0.002
PE–CAP	4.55 ± 0.02	—	—	0.071 ± 0.004	0.042 ± 0.002
M-PE–CAP	1.56 ± 0.01	—	—	0.071 ± 0.004	0.062 ± 0.003
PE–CAB	5.58 ± 0.03	—	—	0.055 ± 0.003	0.033 ± 0.002
M-PE–CAB	1.74 ± 0.02	—	—	0.072 ± 0.004	0.061 ± 0.003

[a] Extraction of the polyolefin phase with xylene.
[b] Intensity ratio obtained before and after extraction by Raman spectroscopy (see the text for details).

surements before and after extraction with a selective solvent, as shown in Table III. Initially, all composites present 80 wt % polyolefin and 20 wt % polysaccharide. In the case of the PE–CEL and M-PE–CEL composites, the polyolefin chains are extracted with xylene, which dissolves both PE and M-PE but does not dissolve CEL chains. In the absence of MA, the polyolefin chains are fully extracted. In contrast, in the case of M-PE–CEL, only 74 wt % is removed, whereas 6 wt % remains attached to the CEL phase. This means that in the interfacial region, where M-PE and CEL are intimately bound, xylene is inert. Similar effects have been observed for composites of crystalline CEL and maleated polyethylene.[32] As the composites prepared with CA, CAP, and CAB, acetone is used to extract the polysaccharide. Acetone does not dissolve PE or M-PE; it dissolves only the cellulose ester. In the absence of MA, the amounts extracted from PE–CA, PE–CAP, and PE–CAB are 6.66, 4.55, and 5.58 wt %, respectively. However, in the case of composites prepared with M-PE, the contents of the extracted polysaccharide are reduced. Particularly in the case of M-PE–CAP and M-PE–CAB, the extracted amounts drop to 1.56 and 1.74 wt %, respectively, indicating that the interfacial phase composed of M-PE and cellulose ester cannot be dissolved by acetone. These findings yield evidence affirming that MA plays an important role in the interfacial adhesion between the matrix and the polysaccharide. Therefore, polysaccharides with a large number of hydroxyl groups per monomer interact more strongly with M-PE.

Raman spectra have been acquired for all composites before and after extraction with a selective solvent. To exemplify this procedure, Figure 6 shows typical Raman spectra obtained for M-PE, CAP, and the M-PE–CAP composite before and after extraction with acetone. In the case of the PE–CEL and M-PE–CEL composites, for which the polyolefin chains have been extracted, the intensity ratio I_{1373}/I_{14406} increases after extraction, corroborating the gravimetric results. In the case of composites prepared with M-PE and CAP or CAB, the intensity ratio I_{1740}/I_{1440} after extraction remains practically the same. These findings come along with the small amounts of material extracted with the selective solvents in both cases. In the case of composites prepared with PE, I_{1740}/I_{1440} decreases after extraction, showing that in the absence of MA, cellulose esters can be more easily removed.

CEL, CA, CAP, and CAB are semicrystalline or amorphous polymers, as evidenced by XRD measurements in Figure 7(a–d), respectively. Zhang et al.[15] recently argued that fillers with low crystallinity favor compatibility in composites, and this can explain the superior mechanical properties of the systems with CAP and CAB, which are less crystal-

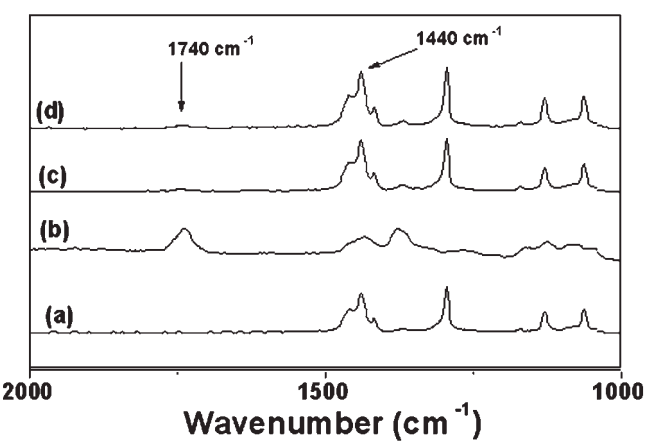

Figure 6 Raman spectra obtained for (a) M-PE, (b) CAP, (c) the M-PE–CAP composite before extraction with acetone, and (d) the M-PE–CAP composite after extraction with acetone.

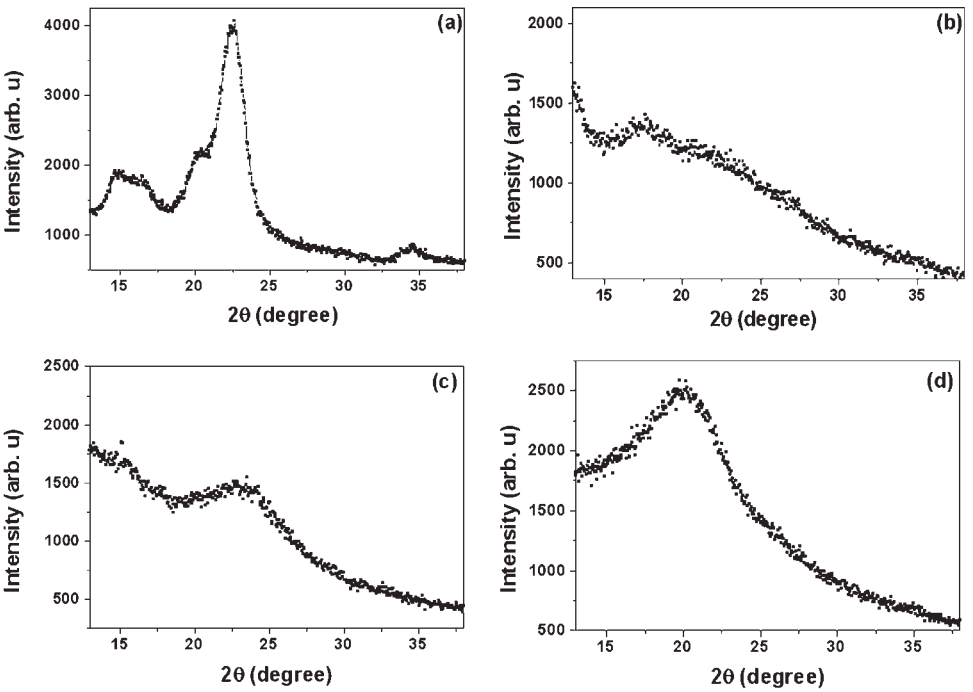

Figure 7 X-ray diffractograms obtained for (a) CEL, (b) CA, (c) CAP, and (d) CAB.

line materials. XRD studies have been carried out for the PE–polysaccharide and M-PE–polysaccharide composites in an effort to obtain additional information on the miscibility. Diffraction peaks and amorphous halos are typical features of semicrystalline polymers. Polyethylene crystallizes in the all-trans conformation and belongs to the orthorhombic crystal class. The corresponding lattice constants[33] are $a = 0.742$ nm, $b = 0.495$ nm, and $c = 0.254$ nm. All diffractograms have been decomposed according to Lorentzian function fits to quantify the area corresponding to the (110) and (200) diffraction peaks and the amorphous halo, as exemplified in Figure 8(a) for original PE. Figure 8(b) shows typical curves of X-ray scattering as a function of the scattering angle obtained for M-PE–CAP. The diffraction peaks at 21.5 and 23.8° (Table IV) correspond to the (110) and (200) diffraction planes, respectively.[11,12,25,33,34]

The interplanar spacing (d_{hkl}) has been determined with Bragg's equation:

$$d_{hkl} = \lambda/(2 \sin \theta_{hkl}) \quad (1)$$

where θ_{hkl} is half of the diffraction angle of the (hkl) atomic plane and λ is the wavelength of the X-ray.

The characteristic lattice constants a and b determined from d_{hkl} and the Miller indices are 0.75 and 0.52 nm, respectively. These values are identical to

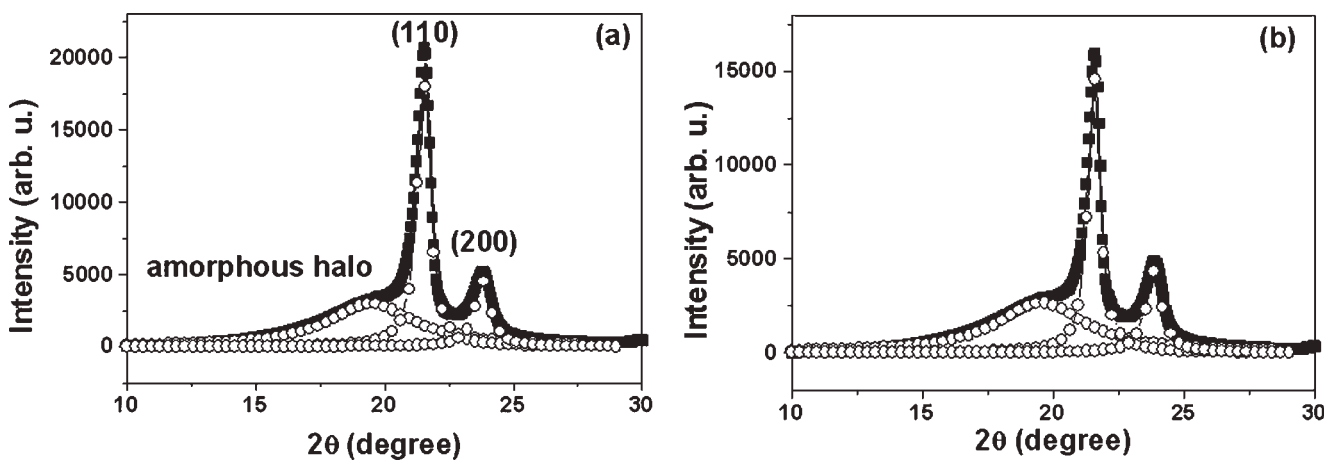

Figure 8 X-ray diffractograms obtained for (a) neat PE and (b) the M-PE–CAP composite with curve decompositions following Lorentzian function fits.

TABLE IV
Areas Corresponding to the (110) and (200) Diffraction Peaks and the Amorphous Halo, Peak Positions, and DC Values

	Area (au)[a]			Peak Position (°)		
Sample	(110)	(200)	Amorphous halo	(110)	(200)	DC (±1%)
PE	17.5	5.2	19.0	21.5	23.8	54
M-PE	16.3	6.9	19.6	21.5	23.8	54
PE–CEL	13.0	5.6	21.4	21.5	23.8	47
PE–CA	12.8	4.8	16.5	21.5	23.8	52
PE–CAP	12.7	4.8	17.1	21.5	23.8	51
PE–CAB	12.2	5.2	16.4	21.4	23.7	51
M-PE–CEL	13.6	5.8	20.6	21.5	23.8	46
M-PE–CA	12.7	4.6	17.0	21.5	23.8	50
M-PE–CAP	12.2	4.5	17.0	21.5	23.8	49
M-PE–CAB	12.3	5.2	17.2	21.5	23.8	51

[a] From the decomposition following the Lorentzian fits.

those reported for polyethylene,[33] indicating that the orthorhombic crystal class remains after processing. The diffractograms in Figure 8 are characterized by the presence of an amorphous halo and two diffraction peaks. The degree of crystallinity (DC) has been calculated as follows:

$$\text{DC}\ (\%) = [A_c/(A_c + A_a)] \times 100 \qquad (2)$$

where A_a and A_c correspond to the areas calculated for the amorphous and crystalline region.[25,35] The DC value found for PE and M-PE samples is 54% (Table IV). After PE is mixed with CEL, CA, CAP, and CAB, the DC values decrease to 46, 52, 51, and 51%, respectively. In the case of composites prepared with M-PE, the decrease in DC is more pronounced when CEL (46%) or CAP (49%) is used. One should be aware that these calculations result from Lorentzian function fits and should be taken as indicative of a tendency. The tendencies here show that regardless of the type of polysaccharide, a decrease in the DC values has been observed. However, this effect is stronger in M-PE–CEL and M-PE–CAP, for which the highest σ_y and E' values have been observed. Nevertheless, the lattice constants have not been affected by the processing because no change in the (110) and (200) peak positions has been observed.

CONCLUSIONS

Composites have been prepared with PE or M-PE and four different polysaccharides—CEL, CA, CAP, and CAB. The structures and properties of the composites and the compatibilizing effect of MA on the interfacial adhesion have been studied with different experimental techniques. The main results can be described as follows:

- The highest σ_y values have been observed for composites prepared with M-PE and CEL or CAP, which carries the highest hydroxyl content per chain.
- M-PE–CAP and M-PE–CAB composites present the highest ε_b values.
- DMTA measurements obtained for composites composed of M-PE and CAP reveal the appearance of a relaxation, which can be attributed to a miscible phase. The high E' value obtained for M-PE–CAP suggests strong interfacial adhesion between M-PE and CAP.
- The decrease in DC, as determined by XRD, is more pronounced in the case of M-PE–CEL and M-PE–CAP. The addition of CEL, CA, CAP, or CAB has no influence on the lattice constants or on the T_m values determined for PE or M-PE by XRD and DSC, respectively.
- The extraction of one component with a selective solvent followed by gravimetry and Raman spectroscopy yields quantitative evidence confirming the compatibilizing effect of MA on the composites, especially those prepared with CAP and CAB.

An esterification reaction between the —COOH and —C=O groups grafted onto M-PE and the hydroxyl functionality on the polysaccharides takes place, leading to composites with superior performance. Therefore, composites prepared with CEL or CAP, which has the highest number of hydroxyl groups per monomer (degree of substitution for hydroxyl = 0.5), are potential composites for practical purposes. However, in the absence of MA, the composites present a poor performance, which indicates that the dispersive forces between the hydrophobic polyolefin phase and the cellulose ester alkyl residues play a marginal role in the interfacial adhesion.

The authors acknowledge Sérgio D. Almeida (Politeno, SP) for supplying the polyolefin samples and Eastman Chemical Co. for supplying the cellulose ester samples.

References

1. Wambua, P.; Ivens, J.; Verspoet, I. Compos Sci Technol 2003, 63, 1259.
2. Joshi, S. V.; Drzal, L. T.; Mohanty, A. K.; Arora, S. Compos A 2004, 35, 371.
3. Toriz, G.; Arvidsson, R.; Westin, M.; Gatenholm P. J Appl Polym Sci 2003, 88, 337.
4. Zafeiropoulos, N. E.; Williams, D. R.; Baillie, C. A.; Matthews, F. L. Compos A 2002, 33, 1083.
5. Weollerdorfer, M.; Bader, H. Ind Crops Prod 1998, 8, 105.
6. Liu, W.; Wang, Y. J.; Sun, Z. J Appl Polym Sci 2003, 88, 2904.
7. Pukánszky, B. Eur Polym J 2005, 41, 645.
8. Joseph, P. V.; Joseph, K.; Thomas, S. Compos Interfaces 2002, 9, 171.
9. Castellano, M.; Gandini, A.; Fabbri, P.; Belgacem, M. N. J. Colloid Interface Sci 2004, 273, 505.
10. Beldzki, A. K.; Gassan, J. Prog Polym Sci 1999, 24, 221.
11. Campos, P. G. S.; Fantini, M. C. A.; Petri, D. F. S. J Braz Chem Soc 2004, 15, 532.
12. Casarano, R.; Matos, J. R.; Fantini, M. C. A.; Petri, D. F. S. Polymer 2005, 46, 3289.
13. Yang, C. Q. J Appl Polym Sci 1993, 50, 2047.
14. Colom, X.; Carrasco, F.; Pagés, P.; Cañavate, J. Compos Sci Technol 2003, 63, 161.
15. Zhang, F.; Qiu, W.; Yang, L.; Endo, T.; Hirotsu, T. J Appl Polym Sci 2003, 89, 3292.
16. Marcovich, N. E.; Villar, M. A. J Appl Polym Sci 2003, 90, 2775.
17. Rodríguez, C. A.; Medina, J. A.; Reinecke, H. J Appl Polym Sci 2003, 90, 3466.
18. Park, H.; Misra, M.; Drzal, L. T.; Mohanty, A. K. Biomacromolecules 2004, 5, 2281.
19. Encyclopedia of Polymer Science and Engineering, 2nd ed.; Wiley: New York, 1986; Vol. 16, p 772.
20. http://www.eastman.com (accessed Jan 2006).
21. Moad, G. Prog Polym Sci 1999, 24, 81.
22. Zhang, F.; Endo, T.; Qiu, W.; Yang, L.; Hirotsu, T. J Appl Polym Sci 2002, 84, 1971.
23. Zhandarov, S.; Mader, E. Compos Sci Technol 2005, 65, 149.
24. Balasuriya, P. W.; Ye, L.; Mai, Y.; Wu, J. J Appl Polym Sci 2002, 83, 2505.
25. Kosaka, P. M.; Kawano, Y.; Fantini, M. C. A.; Petri, D. F. S. Macromol Mater Eng 2006, 291, 531.
26. Hristov, V.; Vasileva, S. Macromol Mater Eng 2003, 288, 798.
27. McCrum, N. G.; Read, B. E.; Williams, G. Anelastic and Dielectric Effects in Polymer Solids; Wiley: London, 1967.
28. Amash, A.; Zugenmaier, P. J Appl Polym Sci 1997, 63, 1143.
29. Bikiaris, D.; Aburto, J.; Alric, I.; Borredon, E.; Botev, M.; Betchev, C.; Panayiotou, C. J Appl Polym Sci 1999, 71, 1089.
30. Dascalu, M. C.; Vasile, C.; Silvestre, C.; Pascu, M. Eur Polym J 2005, 41, 1391.
31. Wolfram, J.; Ehrenstein, G. W.; Avondel, M. A. J Therm Anal Calorim 1999, 56, 1147.
32. Zhang, F.; Qiu, W.; Yang, L.; Endo, T.; Hirotsu, T. J Mater Chem Commun 2002, 12, 24.
33. Elias, H. G. An Introduction to Polymer Science, 1st ed.; VCH: New York, 1997.
34. Hu, S.-R.; Kyu, T.; Stein, R. S. J Polym Sci Part B: Polym Phys 1987, 25, 71.
35. Encyclopedia of Polymer Science and Engineering, 2nd ed.; Wiley: New York, 1986; Vol. 4, p 494.